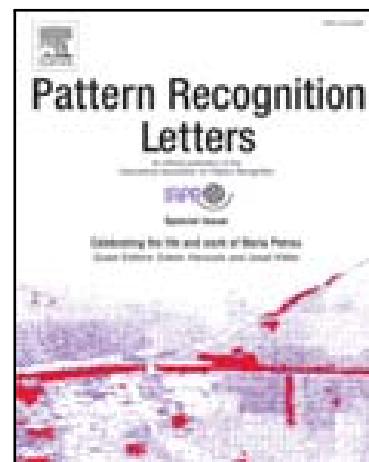# Accepted Manuscript

Rotation Invariant Texture Descriptors based on Gaussian Markov Random Fields for Classification

Chathurika Dharmagunawardhana, Sasan Mahmoodi, Michael Bennett, Mahesan Niranjan

Please cite this article as: Chathurika Dharmagunawardhana, Sasan Mahmoodi, Michael Bennett, Mahesan Niranjan, Rotation Invariant Texture Descriptors based on Gaussian Markov Random Fields for Classification, *Pattern Recognition Letters* (2015), doi: 10.1016/j.patrec.2015.10.006

Highlights

- Rotation invariant descriptors based on Local Parameter Histograms are proposed.

- Two approaches are suggested which produce RI-LPH and I-LPH descriptors.

- RI-LPH descriptor is formulated by circular shifting the neighbour values.

- I-LPH descriptor is generated using isotropic Gaussian Markov Random Fields.

- Both descriptors achieve higher classification accuracies in invariant texture analysis.

Rotation Invariant Texture Descriptors based on Gaussian Markov Random Fields for Classification

Chathurika Dharmagunawardhana[a,**], Sasan Mahmoodi[a], Michael Bennett[b,c], Mahesan Niranjan[a]

[a]Building 1, School of Electronics and Computer Science, University of Southampton, Southampton, SO17 1BJ, UK
[b]Faculty of Medicine, University of Southampton, Southampton General Hospital, Southampton, UK
[c]National Institute for Health Research, Southampton Respiratory Biomedical Research Unit, University Hospitals Southampton NHS Foundation Trust, Southampton, UK

ABSTRACT

Local Parameter Histograms (LPH) based on Gaussian Markov random fields (GMRFs) have been successfully used in effective texture discrimination. LPH features represent the normalized histograms of locally estimated GMRF parameters via local linear regression. However, these features are not rotation invariant. In this paper two techniques to design rotation invariant LPH texture descriptors are discussed namely, Rotation Invariant LPH (RI-LPH) and the Isotropic LPH (I-LPH) descriptors. Extensive texture classification experiments using traditional GMRF features, LPH features, RI-LPH and I-LPH features are performed. Furthermore comparisons to the current state-of-the-art texture features are made. Classification results demonstrate that LPH, RI-LPH and I-LPH features achieve significantly better accuracies compared to the traditional GMRF features. RI-LPH descriptors give the highest classification rates and offer the best texture discriminative competency. RI-LPH and I-LPH features maintain higher accuracies in rotation invariant texture classification providing successful rotational invariance.

1. Introduction

Texture feature extraction mainly aims at formulating efficient discriminative texture descriptors (Petrou and Sevilla, 2006; Tuceryan and Jain, 1998). Texture analysis has been extensively studied in recent years and a large number of texture feature extraction techniques have been developed (Cohen et al., 1991; Nixon and Aguado, 2008; Varma and Zisserman, 2009; Zhao et al., 2012; Chen et al., 2010; Liu and Fieguth, 2012; Lei et al., 2014; Qi et al., 2012; Hinton and Salakhutdinov, 2006; Cimpoi et al., 2014; Simonyan et al., 2014). These methods can be roughly grouped into four main categories, namely statistical, structural, spectral and model based feature extraction methods (Xie and Mirmehdi, 2008).

Model based methods use generative models to represent images, with the estimated model parameters as texture features. GMRF is a popular model based texture feature extrac-

tion scheme with an analytically and computationally efficient parameter estimation process (Tuceryan and Jain, 1998). The parameter estimation is achieved via Least Square Estimation (LSE). The model parameters of GMRF model, also known as traditional GMRF (TGMRF) descriptors, have been employed in successful texture classification and segmentation (Chellappa and Chatterjee, 1985; Manjunath and Chellappa, 1991; Xia et al., 2006b,a; Mahmoodi and Gunn, 2011). TGMRF features describe spatial pixel dependencies which is a primary characteristic associated with texture. However, these features ignore some important structural and statistical information about the texture and have performed poorly (Ojala et al., 2001; Hadjidemetriou et al., 2003; Pietikäinen et al., 2000; Petrou and Sevilla, 2006; Liu and Wang, 2003). Therefore in recent work, we proposed Local Parameter Histogram (LPH) descriptor which is an improved texture descriptor demonstrating significant improvement in characterizing texture compared to the TGMRF descriptors (Dharmagunawardhana et al., 2014b) .

LPH descriptors however, are not rotation invariant. Thus, in this paper our main contribution is to achieve rotation invariant texture features based on LPH descriptors. Rotation

---
[**]Corresponding author: Tel.: +44 (0)23 8059 8867; fax: +44 (0)23 8059 4498;

e-mail: cd6g10@ecs.soton.ac.uk (Chathurika Dharmagunawardhana)

invariant texture features are primarily required when the considered texture instances are comprised of rotated versions of the original texture. These type of scenarios can be found in many applications, for example, in medical image texture, in natural image texture as well as in synthetically produced rotation variant texture database classification. We introduce two new rotation invariant texture descriptors known as Rotation Invariant LPH (RI-LPH) features and Isotropic LPH (I-LPH) features. RI-LPH descriptors are suitable for directional texture analysis while I-LPH descriptors are ideal for isotropic texture description. RI-LPH descriptors are constructed using a local circular neighbourhood shifting process and I-LPH features are based on Isotropic GMRFs (IGMRFs). Furthermore, this paper illustrates comparative generalized classification performance of TGMRF, LPH, RI-LPH and I-LPH descriptors and comparisons to the current state-of-the-art texture descriptors.

This paper is organized as follows. Section 2 and section 3 briefly explain the TGMRF features and LPH descriptors respectively. Section 4 introduces the rotation invariant texture descriptors and in section 5 results and discussions are presented. Finally the conclusions are given in section 6.

2. Traditional GMRF (TGMRF) Descriptors

Let $\Omega = \{s = (i, j) | 1 \le i \le H, 1 \le j \le W\}$ represent the set of grid points on a regular lattice corresponding to an image region of size $H \times W$ which is pre-processed to have zero mean. The intensity value of the pixel at the location s is given by y_s and N denotes the set of relative positions of its neighbours. For simplicity only the square neighbourhoods of size $n \times n$ pixels are used here for N and n is a positive odd integer value. Then the local conditional probability density function of GMRF is given by,

$$p(y_s | y_{s+r}, r \in N) = \frac{1}{\sqrt{2\pi\sigma^2}} \exp \left\{ -\frac{1}{2\sigma^2} \left(y_s - \sum_{r \in \tilde{N}} \alpha_r \bar{y}_{s+r} \right)^2 \right\} \tag{1}$$

where $\bar{y}_{s+r} = (y_{s+r} + y_{s-r})$. The pixels in symmetric positions about the pixel s are assumed to have identical parameters (Petrou and Sevilla, 2006; Bouman, 2009). i.e. $\alpha_r = \alpha_{-r}$ with $r \in \tilde{N}$ where $\tilde{N}$ is the asymmetric neighbourhood (Zhao et al., 2007). α_r is the interaction coefficient which measures the influence on a pixel by a neighbour intensity value at the relative neighbour position r and the variance parameter σ indicates the roughness of the texture. The model parameters of conditional GMRF model are estimated using LSE. Overlapping $n \times n$ regions sampled from the image region Ω also known as the estimation window, are used to generate sample observations for LSE. In texture classification the Ω region will be same as the entire region of a texture image. The interaction parameters $\alpha = col[\alpha_r | r \in \tilde{N}]$ and variance parameter σ are given by,

$$\alpha = \left[\sum_{s \in \Omega} \bar{y}_s \bar{y}_s^T \right]^{-1} \left[\sum_{s \in \Omega} \bar{y}_s y_s \right] \tag{2}$$

$$\sigma^2 = \frac{1}{|\Omega|} \sum_{s \in \Omega} \left(y_s - \alpha^T \bar{y}_s \right)^2 \tag{3}$$

where vector of neighbour values of y_s located at s is $\bar{y}_s = col[\bar{y}_{s+r} | r \in \tilde{N}]$ and $|\Omega|$ is the number of observations used in the estimation process (Manjunath and Chellappa, 1991; Dharmagunawardhana et al., 2014b). The vector of model parameters, $\mathbf{f} = [\alpha^T, \sigma]^T$ is constant over the domain Ω and has been used to characterize the texture (Chellappa and Chatterjee, 1985; Manjunath and Chellappa, 1991; Mahmoodi and Gunn, 2011). Fig. 1a illustrates the TGMRF feature extraction.

3. Local Parameter Histogram (LPH) Descriptors

Parameter estimation stage of the TGMRF descriptors suffers from producing estimates that are biased and over-smoothed when the GMRF model do not capture the underlying data generating process (Gupta et al., 2008). This reduce the texture discriminative power of TGMRF features. To deal with this, in (Dharmagunawardhana et al., 2014b) we proposed LPH descriptors which produce more descriptive features. LPH feature extraction has two main stages: i) local parameter estimation and ii) histogram construction.

The local parameter estimation stage is similar to the TGMRF parameter estimation, however it is spatially localized to a smaller area Ω_s ($\Omega_s \subset \Omega$) and is carried out at each pixel. In (Dharmagunawardhana et al., 2014b) the spatially localized estimation window, Ω_s is proposed as a square window of size $w \times w$ with w selected as $w = 2n - 1$, where n is the neighbourhood size defined in section 2. The small estimation window Ω_s leads to a small sample size and therefore, the local estimation process may become inconsistent. Tikhonov regularization is applied to find approximate solutions to ill-conditioned problem (Björkström, 2001; Dharmagunawardhana et al., 2014b). Therefore, the local parameter estimates are obtained by minimizing the regularized sum of square local errors and are given by,

$$\alpha_s = \left[\sum_{s \in \Omega_s} \bar{y}_s \bar{y}_s^T + c^2 I \right]^{-1} \left[\sum_{s \in \Omega_s} \bar{y}_s y_s \right] \tag{4}$$

$$\sigma_s^2 = \frac{1}{|\Omega_s|} \sum_{s \in \Omega_s} \left(y_s - \alpha_s^T \bar{y}_s \right)^2 \tag{5}$$

where c is a constant and is called the regularization parameter and I is the identity matrix. By addition of the term $c^2 I$ in equation (4) the inconsistency which may arise from matrix inversion subjected to small sample sizes are alleviated. The model parameter estimates, $\mathbf{f}_s = [\alpha_s^T, \sigma]_s^T$ are depend on the location s and generate spatially varying parameter estimates. Sliding window estimation is used to achieve estimates at each pixel location s. If one of the parameters from the parameter vector, $\mathbf{f}_s$ is considered in the spatial domain, Ω, a parameter image, F_j can be defined as $F_j = \{f_s(j) | s \in \Omega\}$ where $f_s(j) \in \mathbf{f_s}$. The normalized histogram of each parameter image F_j is directly used as the LPH descriptor. The concatenated LPH feature vector is given by,

$$\mathbf{h} = [h(1)^T, \ldots, h(j)^T, \ldots, h((n^2 + 1)/2)^T]^T \tag{6}$$

where $h(j)$ is the normalized LPH of jth parameter image, F_j (Dharmagunawardhana et al., 2014b). Note that $(n^2 + 1)/2$ is
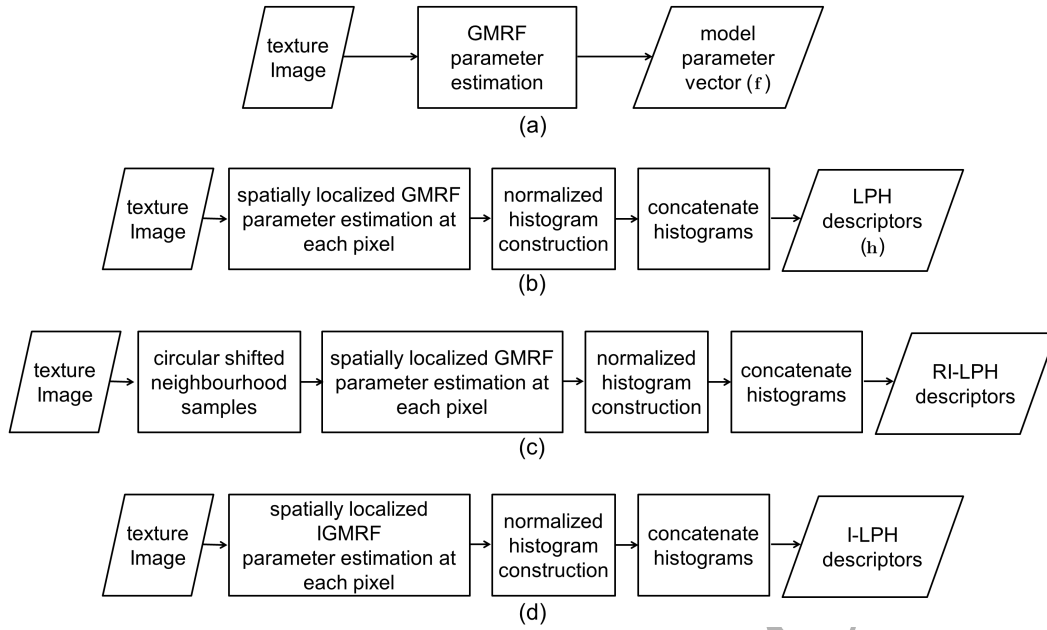
Fig. 1. Construction of (a) TGMRF descriptors, (b) LPH descriptors, (c) RI-LPH descriptors and (d) I-LPH descriptors.

the number of model parameters in $\mathbf{f_s}$ including the variance parameter. Fig. 1b illustrates the LPH feature extraction.

The LPH descriptors can be considered as scale invariant features up to some degree due to the histogram construction. However, they are not rotation invariant.

4. Rotation Invariant Texture Descriptors

Over the last few decades an increased amount of attention has been given to invariant texture analysis, and several methods for achieving the rotation invariance have been proposed. Based on the techniques of achieving rotation invariance, the texture features can be grouped into two main categories namely, rotation invariant directional texture features and omnidirectional texture features.

Rotation invariant directional texture features include texture features that measure directional characteristics of texture, yet are rotation invariant. Discrete Fourier transformation (DFT) is one of the popular choice of achieving rotation invariance. Because the DFT is invariant to translation, by performing DFT on a feature vector containing features from different orientations results in a rotation invariant directional feature. For example, Deng and Clausi (2004) use the DFT of the feature vector obtained from An-isotiopic Circular GMRF (ACGMRF) model as rotation invarient features. In filter based texture feature extraction, after obtaining the responses of directional filters, techniques such as maximum response (Ahonen and Pietikäinen, 2009; Varma and Zisserman, 2005), Fourier transform (Greenspan et al., 1994) or polar transform (Haley and Manjunath, 1995) have been used to achieve rotational invariant features. Polar plots and polarogram is another approach based on polar transformation. Furthermore, feature distributions of locally invariant features such as linear symmetric auto correlation measures, related covariance measures, rotation invariant

local binary patterns and gray level difference have been successfully employed as rotation invariant features (Pietikäinen et al., 2000). The local features are made invariant based on neighbourhood operations such as circular shifting. Unlike, omnidirectional features, these features preserve directional information.

Omnidirectional or isotropic texture features are constructed independent of the direction. The simplest approach of achieving rotation invariance in this way is by using invariant or isotropic statistics such as mean, variance and intensity histogram. Haralick et al. (1973) propose computing omnidirectional features from gray level co-occurrence matrix and Mayorga and Ludeman (1994) employ isotropic texture edge statistics based on circular levels or neighbourhoods. The features extracted from filter responses achieved via isotropic filter kernels have also been proposed and higher texture classification rates have been reported (Porter and Canagarajah, 1997; Zhang et al., 2002). Furthermore, model based approaches such as Circular Simultaneous Auto Regression (CSAR) and its extensions Multiresolution Rotation Invariant Simultaneous Auto Regression (MR-RISAR) model(Kashyap and Khotanzad, 1986; Mao and Jain, 1992) are introduced which employ isotropic model parameters as texture features. The problem with these approaches is that the directionality, an important characteristic of the texture, is lost when an isotropic feature is formulated. Thus, these features are more favourable with isotropic textures. Nevertheless, they are generally computationally less expensive than the rotation invariant directional texture features.

Here we consider two techniques to achieve rotation invariant texture features based on LPH descriptors. These two approaches represent the two categories of rotation invariant features discussed above. Circular neighbourhoods are considered here which are defined by equally spaced neighbour pixel values located on a circle with a radius r. The neighbour values

$$\boldsymbol{y_s} = col[y_{s+r}|r \in N] \qquad \boldsymbol{z_s} = col[z_{s+r}|r \in N]$$
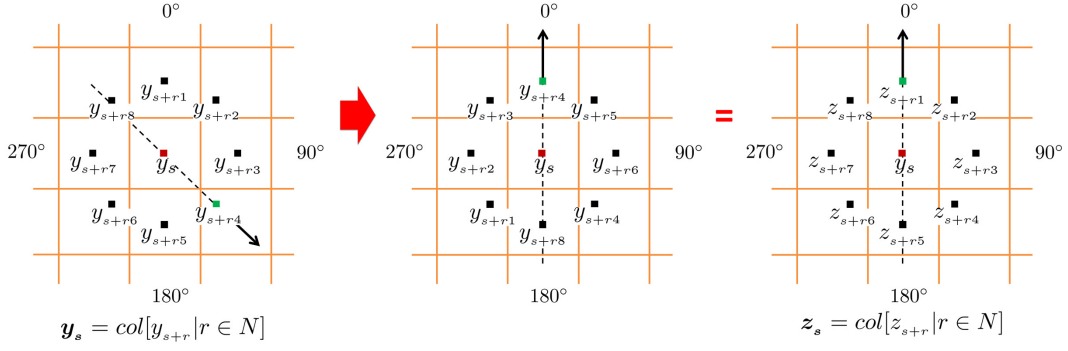
Fig. 2. Rotation invariance by circular shifting.

are calculated using bilinear interpolation similar to Ojala et al. (2002). The number of neighbours in a circle of radius r is referred to by p.

4.1. Circular Shifted Neighbour Method

The rotation invariant features generated by circular shifting the neighbour values are named here as Rotation Invariant LPH (RI-LPH) features. RI-LPH descriptor is a rotation invariant directional texture feature. The neighbour pixel values in the neighbour vector $\tilde{\boldsymbol{y}}_s = col[y_{s+r}|r \in N]$ is circularly shifted based on the neighbour *difference* vector $\boldsymbol{d}_s = col[|y_{s+r} - y_s| \ |r \in N]$. The *difference* value is the absolute difference between a neighbour value and the considered centre pixel. The number of circular shifts to perform is calculated from the $\boldsymbol{d}_s$ by counting the shifts until the first element of the $\boldsymbol{d}_s$ vector becomes the maximum *difference* value. Then the neighbour vector is circularly shifted by that number of shift counts. This process causes rotating the entire circular neighbourhood according to the direction of maximum *difference* value. This leads to a rotation invariant neighbour set $\boldsymbol{z}_s$ at location s. The algorithm for circular shifting neighbours is shown in Algorithm 4.1. The circular shifting process is graphically illustrated in Fig. 2. Subsequently, usual spatially localized LSE process is carried out as in LPH Dharmagunawardhana et al. (2014b). The local parameters estimates can be achieved via the equations (4) and (5) by replacing $\bar{\boldsymbol{y}}_s$ by $\bar{\boldsymbol{z}}_s$ where $\bar{\boldsymbol{z}}_s = col[z_{s+r} + z_{s-r}|r \in \tilde{N}]$.

Algorithm 4.1: Circular Shifting Neighbour Values()

$shiftSize = 1;$
$shiftCount = 0;$
while $\boldsymbol{d}_s(1,1) \neq \max(\boldsymbol{d}_s)$
$\quad$ **do** $\begin{cases} \boldsymbol{d}_s = \text{circShift}(\boldsymbol{d}_s, shiftSize); \\ shiftCount = shiftCount + 1; \end{cases}$
$\boldsymbol{z}_s = \text{circShift}(\tilde{\boldsymbol{y}}_s, shiftCount);$

The estimation window size w is selected similar to the LPH descriptors Dharmagunawardhana et al. (2014b). For a given r, the value of n can be written as $n = 2r + 1$ and therefore, $w = 2n - 1$ becomes $w = 4r + 1$ in terms of r. The differences between associated variables of constructing square neighbourhood based LPH descriptors and the circular neighbourhood

Table 1. Different attributes associated in construction of LPH and RI-LPH descriptors

attribute	LPH	RI-LPH
neighbourhood	square	circular
neighbourhood size	n	(r, p)
estimation window size	$w = 2n - 1$	$w = 4r + 1$
rotation invariance	no	yes

based RI-LPH descriptors are shown in Table 1. After performing localized parameter estimation, the histogram of each parameter image is constructed and concatenated to form the final feature vector. Fig. 1c demostrates the construction process of RI-LPH feature.

4.2. Isotropic GMRF Method

The second approach to achieve rotation invariance is by using IGMRFs, known as Isotropic LPH (I-LPH) descriptors. I-LPH descriptor is an omnidirectional texture feature. IGMRF models the non directional isotropic textures in a simplified GMRF rotational invariant framework with only two model parameters (Kashyap and Khotanzad, 1986; Dharmagunawardhana et al., 2014a). The parameter estimation is simple and fast compared to the GMRF model. IGMRF model is given by,

$$p(y_s|y_{s+r}, r \in N) = \frac{1}{\sqrt{2\pi\sigma^2}} \exp\left\{-\frac{1}{2\sigma^2}\left(y_s - \alpha \sum_{r \in N} y_{s+r}\right)^2\right\} \tag{7}$$

where α and σ are model parameters. At each pixel, the localized LSE process is carried out in a similar way to the RI-LPH descriptors using estimation window of size $w = 4r + 1$. The local parameter estimates are given by,

$$\alpha_s = \frac{\sum_{s \in \Omega_s}\left(y_s \sum_{r \in N} y_{s+r}\right)}{\sum_{s \in \Omega_s}\left(\sum_{r \in N} y_{s+r}\right)^2} \tag{8}$$

$$\sigma_s^2 = \frac{1}{|\Omega_s|}\sum_{s \in \Omega_s}\left(y_s - \alpha_s \sum_{r \in N} y_{s+r}\right)^2 \tag{9}$$

Table 2. Summary of texture datasets used for classification.

dataset name	no. of classes	images per class	total images	image size($pxls$)
BRODATZ	32	20	640	64×64
OUTEX	24	180	4320	128×128
CURET	61	92	5612	200×200

The simple forms of the solutions obtained for model parameters given by (8) and (9) can be easily implemented and efficiently computed. After the parameter estimation, the two parameter images are used to construct the normalized histograms. Fig. 1d illustrates I-LPH feature extraction.

5. Results and Discussion

Texture classification is performed based on three commonly used texture datasets, namely Brodatz (Valkealahti and Oja, 1998; Brodatz, 1996), OUTEX_ TC_ 00000 (Outex Texture Database, 2007) and CURET (Dana et al., 1999). We use BRODATZ, OUTEX and CURET to identify these in subsequent discussion. Each texture dataset represents a good mix of fine to coarse textures. The number of texture classes and samples associated with each dataset is shown in Table 2. All the images are histogram equalized before extracting the texture features. The classification experiments are carried out using k-nearest neighbour (kNN) classifier with $k = 1$ and L1-norm distance metric. The mean and standard deviation of classification accuracies obtained for 100 random splits of equal size training and test sets are reported. Subsequently invariant texture analysis is carried out.

Table 3. Classification accuracies: Comparison with TGMRF descriptors. The mean classification accuracy and the standard deviation achieved from 100 repetitions of classification problem with equal size randomly divided training and test sets.

Dataset	method			
	TGMRF	LPH	RI-LPH	I-LPH
BRODATZ	68.1	92.4	98.0	94.4
	±2.10	±1.55	±1.03	±1.25
OUTEX	79.3	97.6	99.7	99.4
	±2.11	±0.87	±0.11	±0.18
CURET	67.4	89.1	95.6	89.4
	±0.76	±0.53	±0.36	±0.57

5.1. Comparison to TGMRF Descriptors

First the classification accuracy of GMRF based texture descriptors with neighbourhood size is analysed and is given in Fig. 3. Clearly LPH descriptors achieve a significant improvement over TGMRF descriptors. From Fig. 3a,c and e, it can be seen that in general the accuracy increases for three datasets when neighbourhood size n increases with both TGMRF and LPH features. However, roughly after $n = 9$ the accuracy does not increase any more which conveys that low order features
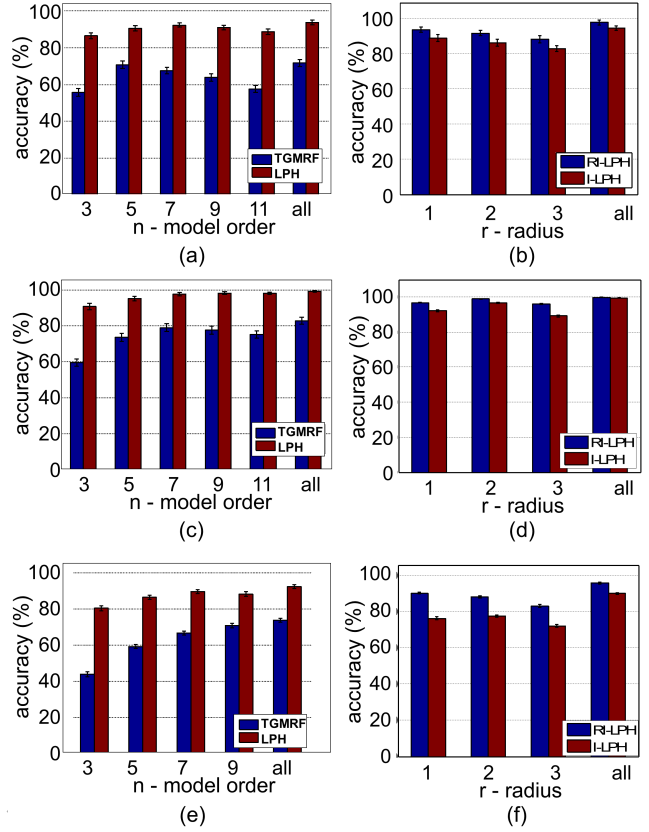
Fig. 3. Texture classification accuracy with model order n and radius r. (a-b) BRODATZ, (c-d) OUTEX, (e-f) CURET dataset. Note that estimation window size, w for TGMRF is the image size [6], for LPH it is $w = 2n - 1$ [16] and for RI-LPH and I-LPH it is based on $w = 4r + 1$ at each level. $p = 8$ is fixed for all levels. Number of bins used for histogram construction is 10.

play a main role in texture characterization. From Fig. 3b,d and f on the other hand, the accuracy slightly decreases or remains unchanged with increasing r for RI-LPH and I-LPH descriptors. This illustrates that nearby neighbour pixels have a higher correlation with the considered pixel relative to the far away neighbours. Therefore it suggests that nearby neighbours are more important for texture feature formulation. However, the rate of accuracy reduction with r is small. Furthermore, Fig. 3 illustrates that RI-LPH descriptors perform better than I-LPH descriptors.
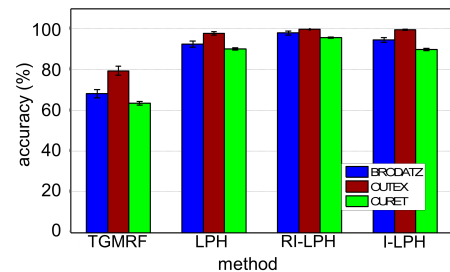

Fig. 4. Texture classification accuracy: Comparison with TGMRF descriptors.

Fig. 3 demonstrates that when the features from different neighbourhoods are integrated, a higher classification accuracy
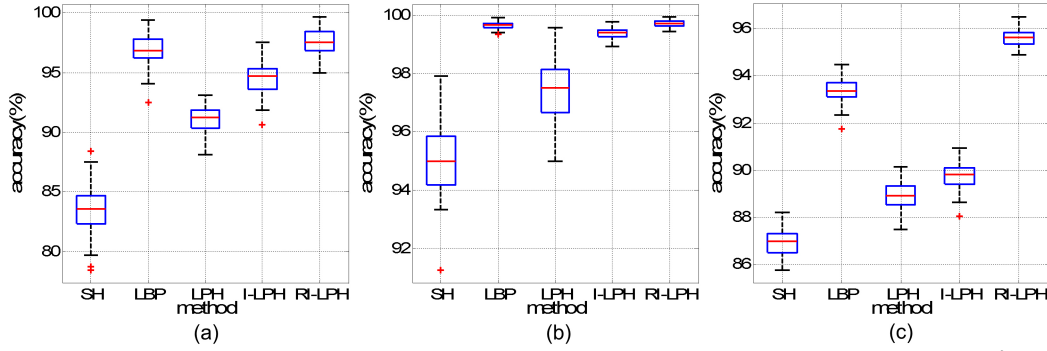
Fig. 5. Texture classification accuracies: Comparison with other texture descriptors. (a) BRODATZ, (b) OUTEX, (c) CURET dataset.

Table 4. Comparison of classification accuracies (%) of some existing texture descriptors with RI-LPH and I-LPH descriptors.

method	dataset	
	BRODATZ	CURET
LBP (Ojala et al., 2002)	97.1	93.3
SH (Liu and Wang, 2003)	84.6	86.4
LBP_HF (Zhao et al., 2012)	97.4	90.6
PRI-CoLBP (Qi et al., 2012)	96.6	99.2
DeCAF (Cimpoi et al., 2014)		97.9
RI-LPH	98.0	95.6
I-LPH	94.4	89.4

can be achieved. Therefore, for RI-LPH and LPH descriptors $r = \{1, 2, 3\}$ feature sets are chosen as the texture descriptors. For TGMRF and LPH however, we are limited to use $n = 7$. This is mainly because when $n = 7$, it gives satisfactory levels of classification accuracies and it is also necessary to consider the computational cost associated with large neighbourhood sizes with many neighbours. Table 3 and Fig. 4 illustrate the classification accuracy of each descriptor under this setting. It is clear that RI-LPH descriptors perform better compared to other features because it is both rotation invariant and well suited for directional textures. Furthermore local parameter distribution based features, LPH, RI-LPH and I-LPH descriptors, are significantly better than TGMRF texture descriptors.

5.2. Comparison to Other Texture Descriptors

In this section, we compare the segmentation performance of proposed features with other standard texture descriptors. The local binary patterns (LBP) is one of the popular state-of-the-art structural texture descriptors in texture analysis (Ojala et al., 2002). Also filter based Gabor texture descriptors are another well known method in texture analysis which closely relates to the biological vision system (Liu and Wang, 2003). These methods have been extensively analysed and used in many studies and applications in image processing and computer vision (Zhang et al., 2002). Some studies have also pointed out that these texture features can perform better than the TGMRF features (Ojala et al., 2001; Hadjidemetriou et al., 2003; Pietikäinen et al., 2000; Liu and Wang, 2003). Therefore, rotational invariant uniform local binary patterns (LBP) (Ojala

et al., 2002) and spectral histograms (SH) (Liu and Wang, 2003) are employed in our study for the comparison. These features represent structural and spectral texture feature domains respectively and are also constructed based on local feature distributions.

Intensity information is not integrated, allowing accuracy comparisons purely based on texture information. The classification accuracies are illustrated in box plots in Fig. 5. According to Fig. 5 RI-LPH features have the best accuracies for all datasets with lowest inter quartile range. I-LPH descriptors demonstrate lower performance than RI-LPH, because I-LPH descriptors ignore directional information and are more suitable for isotropic textures. For SH descriptors a notable reduction of accuracy is observed. This may be the case that the filter set is not optimal, despite the fact that it is a fairly large filter set. However, optimal filter selection is a challenging expensive process. Also we have intentionally avoided using the intensity histogram, which may reduce the performance of SH descriptors. Nevertheless, LBP descriptors perform well for all the three datasets.

More comparisons of classification performance of RI-LPH and I-LPH descriptors with some important texture features are shown in Table 4 . Based on these results we observe that GMRF based RI-LPH and I-LPH features are competitive with other existing texture descriptors. However, PRI-CoLBP shows superior performance on CURET dataset. The difference between the performance of our algorithm and that of PRI-CoLBP for CURET dataset in Table 4 can be explained by noting that in (Qi et al., 2012) colour information is used in their classification, while our simulations are based on purely grey scale images. It is also noted that the SVM classifier used in (Qi et al., 2012) is generally more powerful than the kNN classifier employed here.

In order to analyse the efficiency of each feature extraction method, the time consumption for feature extraction is examined. Here, the time elapsed to extract texture features from a texture image of size 200×200 in a Matlab R2013a environment running on a 2.67 GHz CPU with 12GB RAM is reported. Figure 6 highlights the time consumption comparison. From the Figure 6 it is observed that LPH, RI-LPH and I-LPH descriptors are computationally expensive compared to the other features. This is one of the weaknesses of local parameter distribution based features compared to TGMRF descriptors. Because lo-

cal parameter distribution based features involve local parameter estimation at each pixel and additionally have a histogram construction stage, the computational cost is relatively higher. Nevertheless, the difference between the computation times of TGMRF features and LPH, RI-LPH and I-LPH descriptors are a few seconds. Therefore, the computation of LPH, RI-LPH and I-LPH descriptors are still practically reasonable.

Table 5. Classification accuracies achieved with different rotation angles as the training set (maximum and minimum values are in bold font).

training angle	descriptor		
	LPH	RI-LPH	I-LPH
0°	56.7	94.4	94.2
5°	60.5	94.2	93.9
10°	**61.9**	93.5	94.5
15°	61.7	**95.3**	**94.6**
30°	47.5	95.2	93.9
45°	44.8	90.1	91.4
60°	**43.0**	91.5	92.5
75°	46.8	94.1	89.2
90°	45.4	**89.7**	**82.7**

5.3. Rotation Invariant Analysis

Finally, the performance of rotation invariant texture classification is considered. The OUTEX dataset which has textures from nine different angles namely, 0°, 5°, 10°, 15°, 30°, 45°, 60°, 75° and 90°, is used for this task. Each angle has 20 sample images, hence 180 ($= 9 \times 20$) samples per class (see table 2). The texture samples from one particular angle is used for training and rest of the samples are used for testing. The classification accuracies are shown in Fig. 7 and Table 5. It can be seen from Fig. 7 that RI-LPH and I-LPH descriptors achieve rotational invariance compared to the original LPH descriptors. In general, with the LPH descriptors which are not rotation invariant, the accuracy remains between $40 - 60\%$ across all the tests with different rotation angles for the training set. However, with RI-LPH the accuracy is between $90 - 95\%$ and when I-LPH is used the accuracy is between $80 - 95\%$. Therefore,
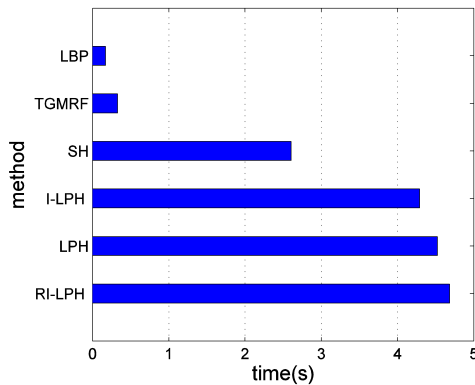

Fig. 6. Time elapsed to extract texture features from a image of size 200×200 **using different texture feature extraction methods.**

RI-LPH and I-LPH descriptors can be employed as rotation invariant texture descriptors.
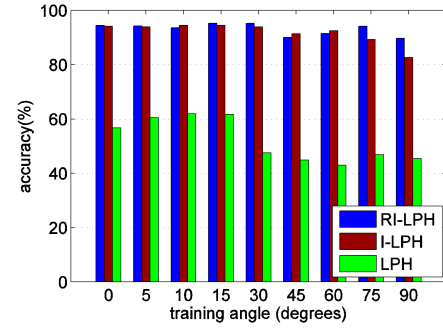

Fig. 7. Classification accuracy with the training angle θ.

6. Conclusions

Two rotation invariant texture descriptors based on LPH features, namely RI-LPH and I-LPH are proposed here for improved texture discrimination. The novel features are tested in texture classification with comparisons to the TGMRF, LPH, LBP and SH texture descriptors. This is the first study that use LPH, RI-LPH and I-LPH features in texture classification. These features demonstrate superior generalized classification performances compared to the TGMRF features on large texture datasets. RI-LPH features gives the best classification rates which also outperform the LBP and SH features. Therefore, RI-LPH features have a higher texture discriminative capability. I-LPH descriptors on the other hand perform better than LPH and SH features. I-LPH features are more suitable for characterizing isotropic textures. Both RI-LPH and I-LPH descriptors proposed here maintain higher classification accuracies in invariant texture analysis and illustrate their rotation invariant abilities in comparison to the LPH descriptors.

References

Ahonen, T., Pietikäinen, M., 2009. Image description using joint distribution of filter bank responses. Pattern Recognition Letters 30, 368–376.

Björkström, A., 2001. Ridge regression and inverse problems. Stockholm University, Department of Mathematics.

Bouman, C.A., 2009. MAP, EM, MRFs, and all that: A user's guide to the tools of model based image and signal processing. https://engineering.purdue.edu/~bouman/ece641/previous/fall08/notes/pdf/Book-header.pdf.

Brodatz, P., 1996. Textures: A Photographic Album for Artists and Designers. New York: Dover.

Chellappa, R., Chatterjee, S., 1985. Classification of textures using Gaussian Markov random fields. IEEE Trans. on Acoustics Speech and Signal Processing 33, 959–963.

Chen, J., Shan, S., He, C., Zhao, G., Pietikainen, M., Chen, X., Gao, W., 2010. Wld: A robust local image descriptor. IEEE Trans. on Pattern Analysis and Machine Intelligence 32, 1705–1720.

Cimpoi, M., Maji, S., Kokkinos, I., Mohamed, S., Vedaldi, A., 2014. Describing textures in the wild, in: IEEE Conf. on Computer Vision and Pattern Recognition, pp. 3606–3613.

Cohen, F.S., Fan, Z., Patel, M.A., 1991. Classification of rotated and scaled textured images using gaussian markov random field models. IEEE Trans. on Pattern Analysis and Machine Intelligence 13, 192–202.

Dana, K.J., Van Ginneken, B., Nayar, S.K., Koenderink, J.J., 1999. Reflectance and texture of real-world surfaces. ACM Transactions on Graphics 18, 1–34.

Deng, H., Clausi, D.A., 2004. Gaussian Markov random field rotation-invariant features for image classification. IEEE Trans. on pattern analysis and machine intelligence 26, 951–5.

Dharmagunawardhana, C., Mahmoodi, S., Bennett, M., Niranjan, M., 2014a. Quantitative analysis of pulmonary emphysema using isotropic Gaussian Markov random fields, in: Proc. of Int'l Conf. on Computer Vision Theory and Applications, pp. 44–53.

Dharmagunawardhana, C., Mahmoodi, S., Bennett, M., Niranjan, M., 2014b. Gaussian Markov random field based improved texture descriptor for image segmentation. Image and Vision Computing 32, 884–895.

Greenspan, H., Belongie, S., Goodman, R., Perona, P., 1994. Rotation invariant texture recognition using a steerable pyramid. Pattern Recognition 2, 162–167.

Gupta, M.R., Garcia, E.K., Chin, E., 2008. Adaptive local linear regression with application to printer color management. IEEE Trans. on Image Processing 17, 936–945.

Hadjidemetriou, E., Grossberg, M.D., Nayar, S.K., 2003. Multiresolution histograms and their use for texture classification, in: Int'l Workshop on Texture Analysis and Synthesis, pp. 1–5.

Haley, G.M., Manjunath, B., 1995. Rotation-invariant texture classification using modified Gabor filters, in: Int'l Conf. on Image Processing, pp. 262–265.

Haralick, R.M., Shanmugam, K., Dinstein, I.H., 1973. Textural features for image classification. IEEE Trans. on Systems, Man and Cybernetics , 610–621.

Hinton, G.E., Salakhutdinov, R.R., 2006. Reducing the dimensionality of data with neural networks. Science 313, 504–507.

Kashyap, R.L., Khotanzad, A., 1986. A model-based method for rotation invariant texture classification. IEEE Trans. on Pattern Analysis and Machine Intelligence 4, 472–481.

Lei, Z., Pietikainen, M., Li, S.Z., 2014. Learning discriminant face descriptor. IEEE Trans. on Pattern Analysis and Machine Intelligence 36, 289–302.

Liu, L., Fieguth, P.W., 2012. Texture classification from random features. IEEE Trans. on Pattern Analysis and Machine Intelligence 34, 574–586.

Liu, X., Wang, D., 2003. Texture classification using spectral histograms. IEEE Trans. on image processing 12, 661–70.

Mahmoodi, S., Gunn, S., 2011. Snake based unsupervised texture segmentation using Gaussian Markov random field models, in: Proc. 18th IEEE Int'l Conf. Image Processing, pp. 1–4.

Manjunath, B.S., Chellappa, R., 1991. Unsupervised texture segmentation using Markov random field models. IEEE Trans. on pattern analysis and machine intelligence 13, 478–482.

Mao, J., Jain, A.K., 1992. Texture classification and segmentation using multiresolution simultaneous autoregressive models. Pattern recognition 25, 173–188.

Mayorga, M.A., Ludeman, L.C., 1994. Shift and rotation invariant texture recognition with neural nets, in: IEEE Int'l Conf. Neural Networks, pp. 4078–4083.

Nixon, M., Aguado, A., 2008. Feature extraction & image processing. 2nd ed., Academic Press.

Ojala, T., Pietikainen, M., Maenpaa, T., 2002. Multiresolution gray-scale and rotation invariant texture classification with local binary patterns. IEEE Trans. on pattern analysis and machine intelligence 24, 971–987.

Ojala, T., Valkealahti, K., Oja, E., Pietikäinen, M., 2001. Texture discrimination with multidimensional distributions of signed gray-level differences. Pattern Recognition 34, 727–739.

Outex Texture Database, 2007. Texture classification test suites, center for machine vision research, University of Oulu. http://www.outex.oulu.fi/index.php?page=classification.

Petrou, M., Sevilla, P.G., 2006. Image Processing, Dealing with Texture. John Wiley & Sons Ltd.

Pietikäinen, M., Ojala, T., Xu, Z., 2000. Rotation-invariant texture classification using feature distributions. Pattern Recognition 33, 43–52.

Porter, R., Canagarajah, N., 1997. Robust rotation-invariant texture classification: wavelet, Gabor filter and GMRF based schemes, in: IEE Proc. Vision, Image and Signal Processing, pp. 180–188.

Qi, X., Xiao, R., Guo, J., Zhang, L., 2012. Pairwise rotation invariant co-occurrence local binary pattern, in: European Conference on Computer Vision, pp. 158–171.

Simonyan, K., Vedaldi, A., Zisserman, A., 2014. Learning local feature descriptors using convex optimisation. IEEE Trans. on Pattern Analysis and Machine Intelligence 12, 25–70.

Tuceryan, M., Jain, A.K., 1998. Texture analysis, in: Handbook of Pattern Recognition and Computer Vision. 2nd ed.. chapter 2.1, pp. 207–248.

Valkealahti, K., Oja, E., 1998. Reduced multidimensional co-occurrence histograms in texture classification. IEEE Trans. on Pattern Analysis and Machine Intelligence 20, 90–94.

Varma, M., Zisserman, A., 2005. A statistical approach to texture classification from single images. International Journal of Computer Vision 62, 61–81.

Varma, M., Zisserman, A., 2009. A statistical approach to material classification using image patch exemplars. IEEE Trans. on pattern analysis and machine intelligence 31, 2032–2047.

Xia, G., He, C., Sun, H., 2006a. Urban extraction from SAR images using local statistical characteristics and Gaussian Markov random field model, in: Proc. 8th IEEE Int'l Conf. Signal Processing, pp. 20–23.

Xia, Y., Feng, D., Zhao, R., 2006b. Adaptive segmentation of textured images by using the coupled Markov random field model. IEEE Trans. on Image Processing 15, 3559–3566.

Xie, X., Mirmehdi, M., 2008. A galaxy of texture features. Handbook of texture analysis , 375–406.

Zhang, J., Tan, T., Ma, L., 2002. Invariant texture segmentation via circular Gabor filters, in: Proc. 16th Int'l Conf. Pattern Recognition, pp. 901–904.

Zhao, G., Ahonen, T., Matas, J., Pietikainen, M., 2012. Rotation-invariant image and video description with local binary pattern features. IEEE Trans. on Image Processing 21, 1465–1477.

Zhao, Y., Zhang, L., Li, P., Huang, B., 2007. Classification of high spatial resolution imagery using improved Gaussian Markov random-field-based texture features. IEEE Trans. on Geoscience and Remote Sensing 45, 1458–1468.